ГЛАСНИК Српског географског друштва 104(2) 213-228
BULLETIN OF THE SERBIAN GEOGRAPHICAL SOCIETY 2024

Original scientific paper
UDC 551.582:624.136(65)
https://doi.org/10.2298/GSGD2402213S

Received: July 20, 2024
Corrected: September 09, 2024
Accepted: October 05, 2024

Sara Sahnoune[1*], Sarah Benharkat[*], Abderahim Kouloughli[**]

** Laboratory of Bioclimatic Architecture & Environment, Faculty of Architecture and Urban Planning, University of Constantine 3 Salah Boubnider, Constantine, Algeria*
*** Institute of Urban Technology Management, Department of City Management and Urbanization, University of Constantine 3 Salah Boubnider, Constantine, Algeria*

SPATIOTEMPORAL COOLING EFFICIENCY ANALYSIS OF WATER STRUCTURES: A CASE STUDY OF THE BENI-HAROUN DAM, ALGERIA

Abstract: Water cool Islands (WCIs) are a key strategy for mitigating Surface Urban Heat Islands (SUHIs) despite the characteristic limitations of water bodies. This paper reports an analysis of the spatial and temporal variation in Surface Urban Heat Island (SUHI) intensity in the Mila region of Algeria, with a focus on evaluating Water Cool Island's (WCI) effectiveness of the country's largest and most substantial hydraulic infrastructure, the Beni-Haroun Dam. Landsat 5TM and Landsat 8 OLI/TIR imagery from 1991 to 2022 were required and analyzed during the hottest and driest periods. Additionally, a comprehensive assessment of the Weighted Normalized Difference Water Index (WNDWI) was conducted, followed by classification and mapping using ArcGIS 10.8. The findings demonstrate a significant correlation between the water index and SUHI, with the WNDWI showing the lowest surface temperature values. This resulted a global cooling intensity (WCI= −1.39 °C), translating to a temperature reduction of 1.39°C across study area, with a notable substantial cooling effect observed in the urban areas surrounding the dam. This study underscores the crucial role of water surfaces in mitigating heat islands, offering valuable insights for urban planners seeking to enhance urban climates by modifying existing water surfaces or designing new ones.

Key words: Surface Urban Heat Island (SUHI), Water Cool Island (WCI), Water Index, Remote Sensing Data, Water Bodies Planning

[1] sara.sahnoune@univ-constantine3.dz (corresponding author)
Sara Sahnoune (https://orcid.org/0000-0001-7601-9582)
Sarah Benharkat (https://orcid.org/0009-0004-2798-780X)
Abderahim Kouloughli (https://orcid.org/0009-0005-0010-801X)

Introduction

Surface Urban Heat Islands (SUHIs) are phenomena where urban areas exhibit higher surface temperatures than their suburban areas, significantly impacting the thermal environment. Rapid urbanization, population growth, and alterations in land use through human activities are primarily responsible for the intensification of this phenomenon, as noted in the systematic reviews by Stewart (2011) and Peng et al. (2012). Consequently, evaluating and analyzing SUHI mitigation strategies has become crucial, with Urban Cooling Islands (UCIs) gaining increasing attention among urban researchers.

UCIs are characterized by lower temperatures compared to their immediate surroundings (Chen et al., 2014; Mostofa & Manteghi, 2020), a phenomenon attributed to the cooling effects of green spaces or water bodies, thereby creating Green Cool Islands (GCIs) and Water Cool Islands (WCIs), respectively. Certain Studies (Ghosh & Das, 2018; Yang et al., 2020; Tan et al., 2021; Xie & Li, 2021) highlight that water bodies are more effective in controlling temperature, demonstrating slightly higher cooling intensity and significantly broader cooling ranges compared to green spaces. This enhanced effectiveness is due to the transformation of sensible and latent heat fluxes through increased evaporation rates, leading to significant water effects essential for reducing surface air temperatures in surrounding areas (Sun & Chen, 2012).

To investigate extensive cooling effects of these water bodies, numerous studies (Zhang et al., 2015; Li et al., 2017; Li et al., 2019; Peng et al., 2021) have employed remote sensing techniques utilizing various water indices, such as the Normalized Difference Water Index (NDWI), the Modified Normalized Difference Water Index (MNDWI), and the Weighted Normalized Differential Water Index (WNDWI). Introduced by McFeeters (1996), the NDWI uses the green and Near-Infrared (NIR) bands to detect water changes in vegetation. Xu (2006) adapted the NDWI by replacing the NIR band with the Shortwave Infrared (SWIR) band to form the MNDWI, effectively distinguishing water bodies from urban areas. Further enhancing water detection, Guo et al. (2017) introduced the WNDWI, which combines the NIR and SWIR bands to improve classification accuracy, especially in identifying turbid waters and vegetation in shadowed regions.

These indices are crucial for monitoring how water structures like rivers, lakes, ponds, and reservoirs help mitigate heat and create WCIs. However, factors such as the geometry, depth, and proximity of water bodies significantly influence the intensity of WCIs and the temperature of surrounding surfaces. Notably, the contrast between the impact of larger water bodies and smaller, regularly shaped water bodies within an urban area suggests that larger surface areas produce a more significant cooling effect (Syafii et al., 2017). Moreover, a single larger water body tends to have more substantial temperature effects (Theeuwes et al., 2013; Manteghi et al., 2015; Zhou et al., 2022). Supporting this, a remote-sensing study (Du et al., 2016) conducted in Shanghai, China, which focused on eighteen lakes and three rivers within the city's outer ring road, confirmed that WCIs are more pronounced in lakes than in rivers. This highlights the critical role of water surface depth in mitigating UHI effects. The distance to these lakes also plays a crucial role, as it determines the extent of the cooling effect. Cooling effects up to 800 meters have been observed, significantly impacting the surrounding environment (Ghosh & Das, 2018). Field surveys, such as one conducted in Sheffield, UK, further support this insight,

where the cooling effect from a 22-meter-wide river was noted up to 30 meters from the river banks during the spring and summer seasons (Hathway & Sharples, 2012).

These findings emphasize the interplay of water bodies' characteristics in shaping urban cooling dynamics, which heavily depends on landscape patterns, geographical location, and surrounding land cover (Wu et al., 2020). Accordingly, exploring how large and deep-water structure, such as dams, can reduce SUHI presents a promising pathway. Existing research on dams has primarily focused on their potential impact on soil (New & Xie, 2008), hydrological regimes (Varol et al., 2012), water quality (Abdesselem & Lynda, 2021), biodiversity (Wu et al., 2019), and local communities (Marouf & Remini, 2019), with limited insights into their mesoscale cooling effects on SUHI. Therefore, this research initially focuses on assessing the spatial and temporal variations of SUHI intensity in Mila, Algeria. In conjunction with this, it aims to extract trends and changes over time of the largest hydraulic structure in Algeria, the Beni-Haroun Dam, using the WNDWI to quantify its cooling effect and generate WCI.

Materials and Methods

Study area

The study was conducted in Mila, located in the northeast of Algeria, at coordinates 36°36'N latitude and 6°15'E longitude, with an altitude of 464 m above sea level (Fig. 1).

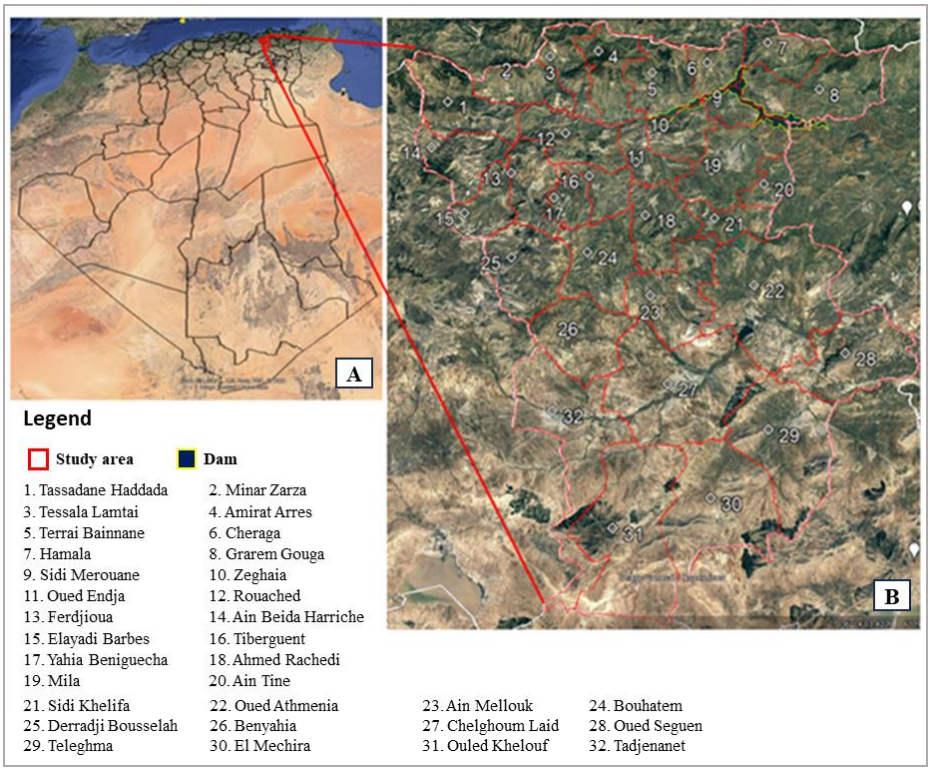

Fig. 1. (A) Location of Mila in Algeria. (B) Administrative division (municipalities) of Mila

Mila is notable for housing the country's most significant hydraulic infrastructure, the Beni-Haroun Dam, covering an area of 52.5 km² and has a capacity of up to 960 million cubic meters. Constructed in 1995 and completed in 2018, the dam was developed to meet the increasing demands for drinking water and irrigation in the semi-arid eastern region of Algeria. In addition to water supply, the Beni-Haroun Dam facilitates flood regulation and hydroelectric power generation.

The study area includes thirty-two (32) urban centers (municipalities), each with varying proximities to the dam. This allows for a meticulous investigation into the relationships between urban environments and their interactions with this significant hydraulic structure.

Climatic data of the study area

The city of Mila is characterized by a semi-humid climate, as defined by the De Martonne (1923) aridity index. This climate features hot, arid summers and cold, rainy winters. As outlined in (Table 1), the mean air temperature reaches its peak at 28.3°C in August, the hottest month, and drops to 9.4°C in January, the coldest month. The mean relative humidity varies significantly throughout the year, ranging from 80% during December and January to 48% in July.

Table 1. Climatic Data for Mila for (1991-2022) (Source: Mila Weather Forecast Centre, 2022)

Data		Jan	Feb	Mas	Apr	May	Jun.	July	Aug	Sept	Oct	Nov	Dec
Temp (°C)	Min	-0.3	-0.06	1.4	3.3	7	11.1	14.9	16.1	12.7	8.5	3.8	0.9
	Avr.	9.4	10.2	13.1	15.7	20	24.6	27.8	28.3	24.6	20.2	14.4	10.5
	Max	19.2	20.6	24.9	28.1	33	38.1	40.6	40.5	36.4	31.9	24.9	20
HR (%)	Min	55	52	49	45	42	34	23	25	37	42	50	55
	Avr.	80	77	74	70	64	56	48	50	62	67	75	80
	Max	105	102	99	95	86	78	73	75	87	92	100	105
Precip (mm)	Avr.	88.2	62.2	65	61.8	49.7	16.4	5.1	16.1	50.7	51.5	76.5	87.7

Data acquisition

The remote sensing data utilized for our study area comprised multi-temporal Landsat images spanning 31 years from 1991 to 2022. These images were obtained freely from the Earth Explorer of the United States Geological Survey (USGS) (https://glovis.usgs.gov/), stipulating that cloud coverage is less than 10%. This data was pivotal in observing the cooling effects of the dam before and after its construction. To cover this extensive timeframe, two satellite images were used: LANDSAT 5 TM Surface Reflectance Tiers for 1991 and 2007, and LANDSAT 8 OLI/TIRS for 2022. These images were explicitly acquired during the hottest month of the year, August, at 10-year intervals to effectively determine the intensity of the SUH and quantify the dam's cooling impact. This period was chosen because the SUHI phenomenon becomes more pronounced and water evaporation reach it peaks, enhancing the cooling effect.

Data processing & analysis

Calculation of surface urban heat Island (SUHI) intensity

To calculate the SUHI intensity, the Mono-window algorithm for LST was initially applied using the thermal bands of Landsat imagery. This process was conducted through the raster calculator in ArcGIS 10.8, based on the metadata file accompanying each satellite

image (Table 2). Specifically, for Landsat 5 (TM), thermal band 6 (10.40 μm-12.50 μm) was utilized, whereas for Landsat 8 (OLI), bands 10 (10.6 μm-11.19 μm) and 11 (11.5 μm-12.51 μm) were employed.

Table 2. Description of Landsat Datasets

Sensors	Date	Hour	Azimuth	Sun Elevation	Path	Raw	Cloud Cover
Landsat 5 (TM)	01 Aout 1991	11:17	107.22400928	59.96683443	194	035	24.0
Landsat 5 (TM)	01 Aout, 2007	10:07	123.78118512	62.12696212	194	035	0.00
Landsat 8 (OLI/TIRS)	10 Aout 2022	10:14	130.37050842	61.50454605	194	035	0.38

The Calculation of the LST from Landsat satellite images involves several key steps. The first step included converting the Digital Numbers (DN) to spectral radiance (Lλ). For the thermal bands of Landsat 5 TM, this conversion is governed by Eq. 1 and Eq. 2 was applied to calculate the spectral radiance (Lλ) for Band 10 for Landsat 8 OLI/ TIRS.

$$L\lambda = (Lmax - Lmin)/(QCALmax - QCALmin) \times (QCAL - QCALmin) + Lmin \quad (1)$$

Where: Lλ = spectral radiance; Lmax = highest spectral radiance; Lmin = lowest spectral radiance; QCALmax = highest DN (255); QCALmin = lowest DN (1); QCAL = DN of Band6.

$$L\lambda = ML \times QCAL + AL \quad (2)$$

Where: Lλ = spectral radiance; ML = multiplicative rescaling factor; QCAL = DN of Band 10; AL = additive rescaling factor

The second step is to convert spectral radiance into brightness temperature (TB) using Eq. 3. and it is converted into ◦C by subtracting 272.15.

$$BT = \frac{(K2)}{Ln}\left(\frac{K1}{L\lambda + 1)}\right) - 272.15 \quad (3)$$

Where: BT = brightness temperature; K1 and K2 = calibrated constants that differ based on sensors; Lλ = spectral radiance.

The third step is to estimate the Land Surface Emissivity (LSE) using the fractional Vegetation cover by the following Eq. 4;

$$E = 0.004 \; ⫽((NIR - R)/(NIR + R) - NDVImin/NDVImax - NDVImin)⫽ \text{^}2 + 0.986 \quad (4)$$

Where: NIR = near-infrared band (Band 5); R= red band (Band 4)

Finally, the resulting LST was obtained using the BT and LSE in the previous steps using Eq. 5;

$$LST = BT/1 + W(BT/p)ln(e) \quad (5)$$

Subsequently, the SUHI, defined as areas with normalized values exceeding one degree (1°C) above the LST average, was calculated by Eq. 6 developed by Zhang (2006).

$$SUHI = Ts - Tm/STD \quad (6)$$

Where: Ts = Land Surface Temperature; Tm = mean Land Surface Temperature of the area; STD= standard deviation.

The intensity of SUHI is quantified using the Urban Thermal Field Variance Index (UTFVI), which assesses the temperature value of each pixel within the urban center relative to the entire region. This index, detailed in Eq. 7, facilitates the classification of environmental quality by comparing thermal variance across the urban landscape (Zhang, 2006).

$$UTFVI = Ts - Tm/Tm \quad (7)$$

Where: Ts= Land Surface Temperature. Tm = mean LST of the area.

The UTFVI values are categorized into six classes, as outlined in (Table 3), which range from none to strongest. These categories reflect the varying intensities of SUHI (Singh et al., 2017).

Table 3. Classification Values of UTFVI (Source: Singh et al., 2017).

Urban Thermal Field Variance Index (UTFVI) range	SUHI Intensity
< 0	None
0–0.005	Low weak
0.005–0.01	Middle
0.01–0.015	Strong
0.015–0.02	Stronger
> 0.02	Strongest

Extraction and mapping of the water index WNDWI

The WNDWI index is calculated by assigning a specific weight to each spectral band based on its water sensitivity and normalizing the difference between the reflectance values of the green b and and the shortwave infrared band, according to the following Eq. 8;

$$WNDWI=(GREEN-a\times NIR-(1-a)\times SWIR)_{x}(GREEN+a\times NIR+(1-a)\times SWIR) \quad (8)$$

Where: GREEN = reflectance value in the green band; NIR = reflectance value in the near-infrared band; SWIR = reflectance value in the shortwave infrared band; a = weighted coefficient, ranging from 0 to 1. If a=0, WNDWI equals the MNDW; If a=1a=1, it equals the NDWI.

For this study, the weighted coefficient a was set to 0.50, as tests have demonstrated that this value ensures high overall accuracy for the index's performance.

Calculation of the Water Cool Island (WCI) effect

The WCI effect is quantified by measuring the temperature difference between water bodies and their surrounding environments. This study calculated WCI as the difference between the average LST of the water surface (LSTw) and the average LST recorded for each urban center (municipality). The formula used is given in Eq. 9;

$$WCI = \Delta LST = LSTw - LSTm \quad (9)$$

Where: LSTw = average LST value within the water class; LSTm = average LST within each urban zone.

The more significant this temperature difference, the stronger the WCI intensity, indicating a more significant cooling effect on the regional surface temperature.

Results

Spatiotemporal dynamics of LST and SUHI intensity

The spatiotemporal dynamics of LST across the analyzed years (1991, 2007, and 2022) reveal significant fluctuations before and after dam construction. These changes are visually represented in (Fig. 2), where a color gradient from blue to red marks the transition from low to high temperatures.

The cooling effects are particularly notable in the vicinity of the dam. For instance, the lowest recorded LST within the dam area was 24.55°C in 2007 and 26.56°C in 2022, indicating a persistent cooling effect despite regional warming trends. In comparison, built-up areas nearby showed only a slight reduction in maximum temperatures from 53.82°C to 53.56°C over the same period. This data underscores the dam's role as a cool island, effectively reducing LST in its immediate surroundings compared to more distant urban areas.

The cooling influence of the dam is also evident in the changing intensity and concentration of red areas on the thermal map, which denotes higher temperatures. While 1991 featured a concentrated and intense red area, indicating higher temperatures, this intensity notably diminished by 2007 and continued to decrease by 2022. This trend suggests that over time, the dam has played a crucial role in mitigating the UHI effect, helping to lower temperatures in the surrounding urban landscape.

Furthermore, the overall trend of changing LST in Mila over the past 30 years reveals a consistent upward trajectory (Table 4). Starting from an average temperature of 36.73°C in 1991, there has been a substantial increase of 6.36°C over three decades, translating to an alarming average rise of approximately 3.47°C per decade. This trend highlights the development of a heat island within the city, characterized by zones of elevated temperatures that starkly contrast with the cooler areas influenced by the dam.

The UTFVI, which assesses the intensity of SUHI and its environmental repercussions, reveals a striking absence of SUHI in the areas adjacent to the dam. In contrast, significant SUHI intensities, ranging from strong to the highest, are predominantly observed in the study area's central, southwest, and southeast sectors, which are distanced from the dam (Fig.3). This disparity underscores the dam's cooling influence on its immediate area, effectively mitigating the SUHI effect in these proximate areas.

However, urban areas further from the dam exhibit enhanced SUHI effects, likely exacerbated by urbanization, the scarcity of green spaces, and increased heat absorption from buildings and pavement. This comprehensive analysis offers a nuanced understanding of the evolving thermal dynamics across the city's urban landscapes, highlighting the dam's significant thermal regulatory role over time.

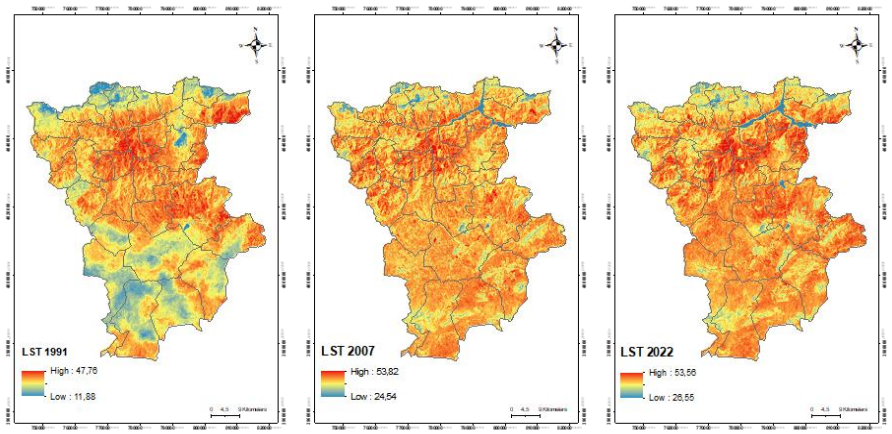

Fig. 2. Spatiotemporal variation of LST from 1991 to 2022

Table 4. Descriptive statistics of LST from 1991 to 2022

LST	1991	2007	2022
LST max	47.76 °C	53.82 °C	53.56 °C
LST avg.	36.73 °C	42.42 °C	43.09 °C
LST min	11.89 °C	24.55 °C	26.56 °C
Standard Deviation	4.07 °C	2.85 °C	3.51 °C
LST changes	1991-2007	2007-2022	1991-2022
LST max	6,06 °C	-0,26 °C	5,80 °C
LST avg.	5,69 °C	0,67 °C	6,36 °C
LST min	12,66 °C	2,01 °C	14.67 °C

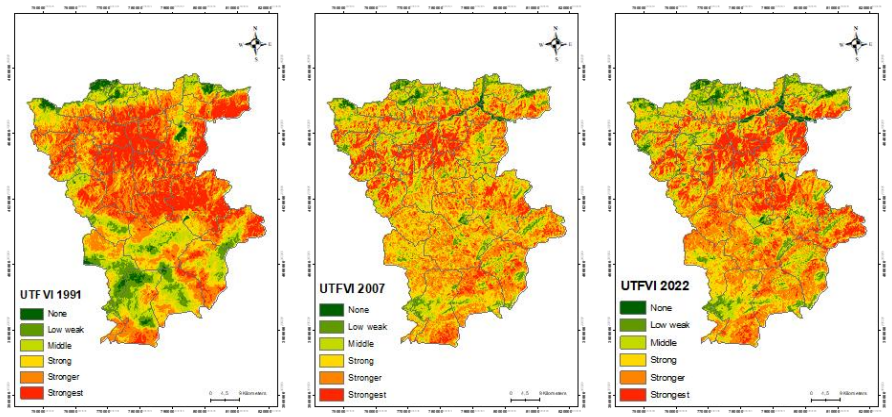

Fig.3. Spatiotemporal variation of the SHIS intensity from 1991 to 2022

Extracting and Changes of water index WNDWI

The temporal evolution of the WNDWI, as represented in (Fig. 4), illustrates significant changes over the study period. The index values ranged from -0.48 to 0.17 in 1991, deepened to -0.60 to 0.53 in 2007, and adjusted to -0.44 to 0.29 in 2022. This progression highlights a remarkable transformation in the area before and after the dam became operational.

Notably, the dam's surface area has shown a consistent annual expansion, exceeding its originally designed capacity by reaching an additional 40 million cubic meters by 2012. In recent years, there has been a substantial increase in the area of the dam. This expansion has preserved the shape of the dam, with the most extensive coverage observed in 2022. This growth signifies the dam's increasing water retention capacity and its evolving role in shaping the regional hydrological landscape.

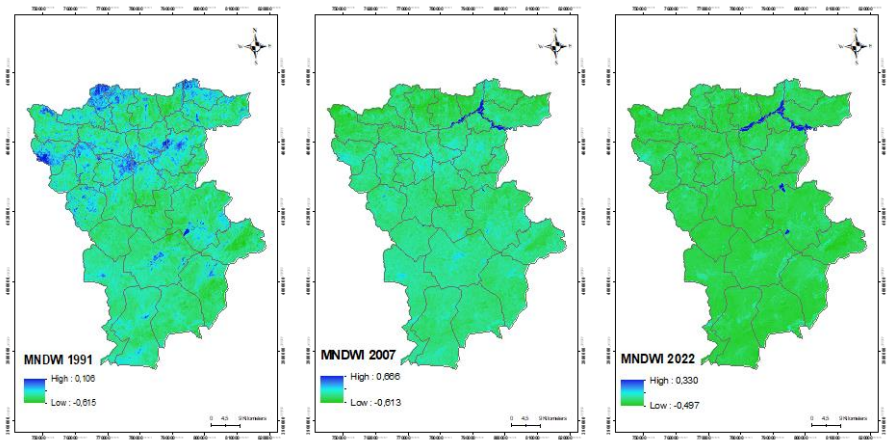

Fig.4. Variations in the WNDWI during the study period (1991, 2007, and 2022)

Estimation of WCI intensity

Table 5 presents the average LST values for each municipality, along with the average temperature of the dam for the years 2007 and 2022, facilitating the computation of the cool island effect's intensity for the dam. The intensity is quantified by the difference between the WCI in 2007 and its effect in 2022. A significant difference between these instances, where one period shows a stronger cooling effect than the other, indicates a more pronounced WCI intensity.

The analysis of the results reveals a substantial cool island effect generated by the dam across all municipalities in Mila. The most pronounced effects were observed in municipalities proximate to the dam, including Minar Zaraza, Tessala Lamtai, Amirat Ares, Terrai Bainnane, Chigara, Hamala, Zeghaia and Elayadi Barbes. Interestingly, some other municipalities farther from the dam also registered a medium intensity of WCI such as, Tassadane Haddada, Grarem Gouga, Ferdjioua and Ain Beida Harriche. This variation in cooling intensity can be attributed to the distance from the dam to the urban centers, with other factors like topography and green areas also playing significant roles in influencing the intensity.

Conversely, the central municipality of Mila recorded the lowest cool island effect, despite its proximity to the dam. This outcome is likely due to the increased urban density in Mila, which has intensified during this period, potentially mitigating the cooling effects of the dam.

Overall, the WCI has effectively lowered the average surface temperature by approximately 1.39 °C compared to the average surface temperature of the entire study area. This substantial reduction confirms the positive impact of the dam in mitigating the SUHI effect.

Table 4. WCI Intensity in each urban center of Mila between 2007 and 2022

Urban Center	LSTm	LSTw_ 2007	WCI_ 2007	LSTm	LSTw_ 2022	WCI_ 2022	ΔWCI
Tassadane Haddada	40,93°C	27,77 °C	-13,16°C	40,97°C	29,22 °C	-11,75°C	1.41°C
Minar Zaraza	42,30°C	27,77 °C	-14,53°C	41,64°C	29,22 °C	-12,42°C	-2.11°C
Tessala Lamtai	39,34°C	27,77 °C	-11,57°C	38,67°C	29,22 °C	-9,46°C	-2.11°C
Amirat Arres	42,67°C	27,77 °C	-12,93°C	39,83°C	29,22 °C	-10,61°C	-2.93°C
Terrai Bainnane	41,75°C	27,77 °C	-13,98°C	40,57°C	29,22 °C	-11,36°C	-2.62°C
Chigara	40,91°C	27,77 °C	-13,14°C	40,81°C	29,22 °C	-11,59°C	-1.55°C
Hamala	40,25°C	27,77 °C	-12,48°C	39,67°C	29,22 °C	-10,46°C	-2.02°C
Grarem Gouga	41,63°C	27,77 °C	-13,86°C	41,92°C	29,22 °C	-12,70°C	-1.16 °C
Sidi Ma-rouene	41,20°C	27,77 °C	-13,43°C	41,80°C	29,22 °C	-12,59°C	-0.84°C
Zeghaia	43,02 °C	27,77 °C	-15,25°C	43,22°C	29,22 °C	-14,01°C	-1.24 °C
Oued Endja	45,21°C	27,77 °C	-17,44°C	46,24°C	29,22 °C	-17,02°C	-0.42°C
Rouached	42,91°C	27,77 °C	-15,14°C	43,44°C	29,22 °C	-14,23°C	-0.91°C
Ferdjioua	42,80°C	27,77 °C	-15,03°C	42,69°C	29,22 °C	-13,47°C	-1.56°C
Ain Beida Harriche	43,80°C	27,77 °C	-16,03°C	43,97°C	29,22 °C	-14,76°C	-1.27°C
Elayadi Barbes	42,67°C	27,77 °C	-14,90°C	42,17°C	29,22 °C	-12,95°C	-1.95°C
Tiberguent	39,34 °C	27,77 °C	-16,47°C	45,87°C	29,22 °C	-16,65°C	0.18°C
Yahia Beniguecha	43,91°C	27,77 °C	-16,14°C	44,88°C	29,22 °C	-15,66°C	-0.78°C
Ahmed Rachdi	43,25°C	27,77 °C	-15,48°C	44,77°C	29,22 °C	-15,55°C	-0.07°C
Mila	42,22 °C	27,77 °C	-14,45°C	44,25 °C	29,22 °C	-15,03°C	0,58°C
Ain Tine	42,46°C	27,77 °C	-14,69°C	44,76°C	29,22 °C	-15,55°C	0.43°C
Sidi Khelifa	41,73°C	27,77 °C	-13,96°C	42,59°C	29,22 °C	-13,38°C	-0.58°C
Oued Atma-nia	42,73°C	27,77 °C	-14,96°C	43,79°C	29,22 °C	-14,58°C	-0.38°C
Ain Melouk	42,73°C	27,77 °C	-14,96°C	44,40°C	29,22 °C	-15,18°C	0.22°C
Bouhatem	42,55°C	27,77 °C	-14,78°C	44,55°C	29,22 °C	-15,33°C	0.55°C
Derradji Bousselah	43,04°C	27,77 °C	-15,27°C	43,73°C	29,22 °C	-14,52°C	-0.75°C
Benyahia	42,67°C	27,77 °C	-14,90°C	44,46°C	29,22 °C	-15,24°C	0.34°C
Chelghoum Laid	42,62°C	27,77 °C	-14,85°C	43,45°C	29,22 °C	-14,24°C	-0.61°C
Oued Seguen	42,53°C	27,77 °C	-14,76°C	44,26°C	29,22 °C	-15,05°C	0.29°C
Teleghma	42,54°C	27,77 °C	-14,77°C	42,81°C	29,22 °C	-13,59°C	-1.18 °C
El Mechira	42,90°C	27,77 °C	-15,13°C	43,25°C	29,22 °C	-14,04°C	-1.09°C
Ouled Khelouf	42,40°C	27,77 °C	-14,63°C	42,84°C	29,22 °C	-13,62°C	-1.01°C
Tadjenanet	42,23°C	27,77 °C	-14,46°C	42,93°C	29,22 °C	-13,71°C	-0.75°C

Discussion

This study comprehensively analyzes the SUHI intensity variation in Mila, Algeria, from 1991 to 2022, using LST and the UTFVI derived from Landsat imagery. Over the years, Mila has witnessed significant land use changes, as reported by (Gherraz et al., 2020), contributing to a notable rise in LST, a phenomenon primarily attributed to increased urbanization and expansion of built-up areas, typically enhanced urban heat due to their low moisture content and heat-retaining materials like concrete and asphalt (Haashemi et al., 2016; Shahfahad et al., 2021). Additionally, reducing vegetation cover and water bodies has further intensified SUHI by diminishing natural cooling sources essential for mitigating urban temperatures (Boudjellal & Bourbia, 2018; Sahnoune et al., 2021).

Intriguingly, despite the steady increase in LST, the rise has not translated into a proportional intensification of SUHI, suggesting a complex interplay between urban development and natural temperature regulation mechanisms (Haashemi et al., 2016). An initial peak in SUHI intensity in 1991 was followed by a noticeable decline in subsequent years, reflecting the potential cooling influence of the Beni-Haroun Dam, constructed post-1991. This pattern is evidenced by the shifts in SUHI levels over the decades, with a marked decrease in higher SUHI levels and an increase in lower levels. Such trends underscore the dam's significant role in moderating local temperatures, thereby contributing to a more moderate urban environment.

The classification of SUHI intensity into five distinct categories: very low, low, moderate, high, and very high (Fig.5) reveals a nuanced understanding of the urban heat landscape.

The percentage of very low SUHI levels increased from 9.50% in 1993 to 6.09% in 2020. Meanwhile, low SUHI levels experienced a slight increase from 48.63% in 1991 to 62.22% in 2007 and then to 63.65% in 2022. Additionally, there was an increase in moderate SUHI levels over the three decades, with the percentage changing from 0% in 1991 to 3.65% in 2007 and then decreasing to 1.32% in 2022. There was a significant decrease in higher SUHI levels from 6.58% in 1991 to 4.02% in 2007 and further to 1.78% in 2022. Similarly, the highest SUHI levels decreased from 39.97% in 1991 to 11.47% in 2007, then increased slightly to 19.52% in 2022. The transformation in SUHI distribution, from a dominance of very high levels in 1991 to an increase in lower SUHI levels by 2022, demonstrates the evolving impact of the dam's cooling effect over time

This study further explored how a dam's presence affects the cooling of each urban center within the study area and the overall reduction in the intensity of the SUHI phenomenon across the entire study area. This relationship is more intuitively illustrated through a vertical cross-section using LST and WNDWI raster data for the years 1991, 2007, and 2022 (Fig. 6).

In 1991, before the dam's construction, the analysis showed no significant correlation between LST and WNDWI, indicating that natural water bodies and terrain features had yet to be significantly altered by human intervention. Post-construction data from 2007 and 2022 revealed a marked change: as the dam's water levels increased, peaks in WNDWI correlated strongly with dips in LST, illustrating the dam's growing efficacy in moderating local temperatures.

The study's results indicate that the enlargement of a dam's surface can significantly amplify the WCI effect. This enhanced cooling capacity is primarily attributed to larger and deep-

er water surfaces which, due to their substantial volume, are capable of absorbing and dissipating more thermal energy. This effectiveness is partly a result of the extended surface area's exposure to direct sunlight. Consistent with findings from (Wu et al., 2020; Bouketta, 2023), these expansive water surfaces serve a dual function: they not only act as thermal energy reservoirs but also promote water convection. This convection plays a critical role in transferring heat away from the water's surface to the air above, facilitating a more even distribution of heat which, in turn, contributes to the reduction of ambient temperatures.

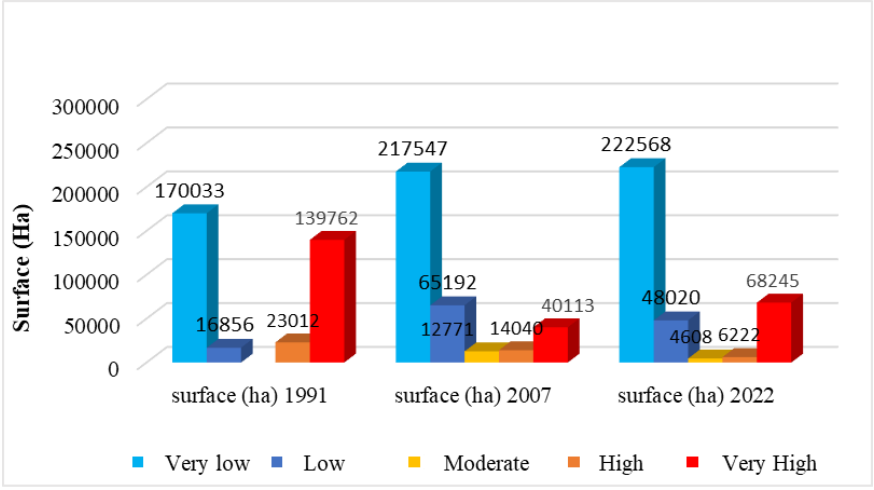

Fig. 5. Temporal evolution of SUHI in relation to the surface area (Ha) from 1991-2022

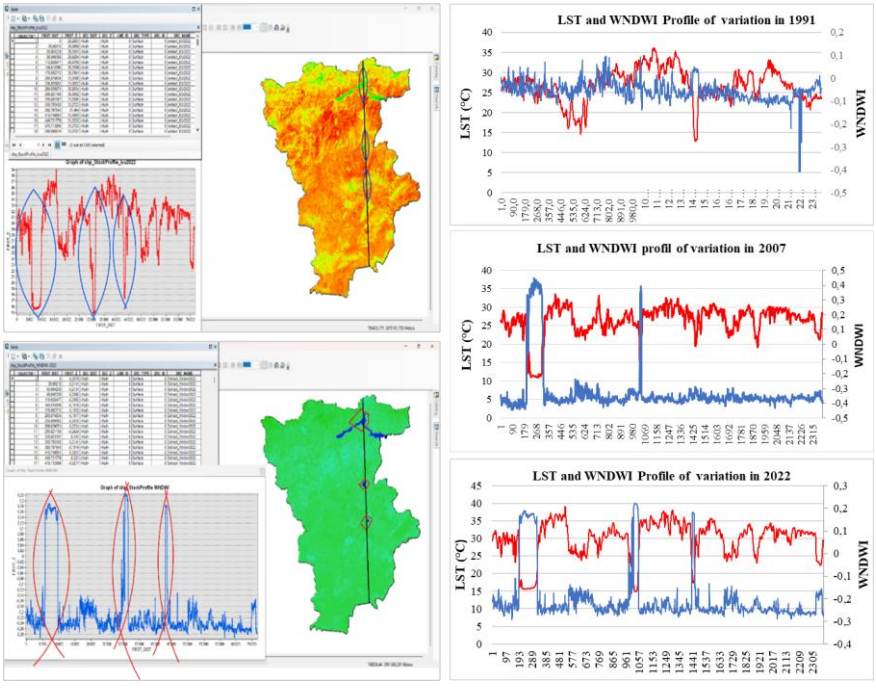

Fig.6. LST and WNDWI profiles of the study area over different years

Moreover, the proximity of urban centers to the dam plays a crucial role in the intensity of the cooling effect experienced. Data indicates that the closer an urban center is to the dam, the stronger the cooling effect it experiences, corroborating studies by (Du et al., 2016; Lee et al., 2016; Cai et al., 2018; Gherraz & Alkama, 2020). This proximity effect underscores the strategic importance of planning urban expansion and infrastructure development in ways that maximize natural and man-made cooling resources.

However, our study also indicates that proximity is not the sole determinant of cooling efficacy. The nature of the surrounding land cover and the frequency of heat exchange between the land and the water surface significantly influence the magnitude of the cooling effect (Wu et al., 2020). Urban areas with high concentrations of heat-absorbing materials like asphalt and concrete might negate some of the cooling benefits, whereas regions with more vegetation can enhance these effects due to the additional shade and transpirational cooling they provide. In terms of practical applications, these insights emphasize the need for urban planners to consider both the placement of water bodies and the surrounding landscape design to optimize natural cooling (Bouketta, 2023). Integrating green infrastructure around water bodies, such as parks and green roofs, can amplify these cooling effects, providing crucial relief in urban heat islands.

Limitations and future directions

While this study has provided valuable insights, future research should focus on more detailed investigations into how urban design, population density, green coverage, and soil characteristics contribute to temperature variations and their interaction with the placement of water bodies and Water Cool Island (WCI) efficiency. Such research is crucial for developing holistic and sustainable approaches to alleviate the adverse effects of rising urban temperatures.

Conclusion

This study comprehensively demonstrates the pivotal role of water surfaces, particularly large-scale dams, in moderating urban temperatures and mitigating the effects of SUHIs. Through the use of remote sensing data and advanced water index (WNDWI) over three decades, we have quantitatively assessed the cooling influence of the Beni-Haroun Dam on the LST and SUHI intensity in Mila, Algeria. Highlights of the study include:

Over the study period, Mila has experienced a progressive increase in the SUHT effect, characterized by a rise in average temperatures of approximately 3.47°C per decade.

The presence of the dam has led to a significant reduction in the LST by 1.39°C within its vicinity, confirming the role of water surfaces as effective natural coolants in urban areas.

There is a clear dynamic relationship between the size of the dam's water surface and the extent of its cooling effects. Notably, the expansion of the dam corresponded with an increased mitigation of the SUHI effect, underscoring the importance of this relationship in the context of global warming and urban development.

Proximity to the dam is critical in maximizing its cooling benefits. Urban centers located closer to the dam experienced more significant temperature decreases, underscoring the importance of strategic urban planning that integrates water bodies close to or within urban developments to capitalize on their cooling effects.

This study has significant implications for urban planning. It underscores the importance of incorporating substantial water bodies into urban designs, which can significantly boost climate resilience and enhance sustainability in urban settings. By carefully positioning these water features and effectively managing the adjacent land uses, urban areas can substantially mitigate heat stress, enhance environmental quality, and promote sustainable growth even as urban areas expand and temperatures rise. On a territorial level and regarding the case study presented, it is essential to preserve and maintain the existing dams., One of the major threats is the silting phenomenon, which endangers the functionality of Algeria's dams. In addition, Algeria's national policy on hydraulic infrastructure development aims to increase water resource mobilization and transfer, particularly in regions suffering from water stress, by building new dams. The future location of these dams should strategically address both the challenges of drought and the consequences of global warming, especially in urban areas. By combining climate resilience with water management in urban and territorial planning, cities can enhance not only their thermal comfort but also their adaptability to future climate challenges.

Conflicts of Interest: The authors declare no conflict of interest.

Publisher's Note: Serbian Geographical Society stays neutral with regard to jurisdictional claims in published maps and institutional affiliations.

References

Boudjellal, L., & Bourbia, F. (2018). An evaluation of the cooling effect efficiency of the oasis structure in a Saharan town through remotely sensed data. *International Journal of Environmental Studies, 75*, 309-320, https://doi.org/10.1080/00207233.2017.1361610

Bouketta, S. (2023). Urban Cool Island as a sustainable passive cooling strategy of urban spaces under summer conditions in Mediterranean climate. *Sustainable Cities and Society, 99*, Article 104956, https://doi.org/10.1016/j.scs.2023.104956

Cai, Z., Han, G., & Chen, M. (2018). Do water bodies play an important role in the relationship between urban form and land surface temperature? *Sustainable cities and society, 39*, 487-498, https://doi.org/10.1016/j.scs.2018.02.033

Chen A., Yao X. A., Sun R. & Chen L., (2014). Effect of urban green patterns on surface urban cool islands and its seasonal variations. *Urban forestry & Urban greening, 13*, 646-654, https://doi.org/10.1016/j.ufug.2014.07.006

De Martonne, E. (1923). Aridité et indices d'aridité. Académie des Sciences. *Comptes Rendus, 182*(23), 1935-1938.

Du, H., Song, X., Jiang, H., Kan, Z., Wang, Z., & Cai, Y. (2016). Research on the cooling island effects of water body: A case study of Shanghai, China. *Ecological indicators, 67*, 31-38, https://doi.org/10.1016/j.ecolind.2016.02.040

Gherraz, H., & Alkama D. (2020). L'estimation de l'impact des espaces verts et des surfaces d'eau sur le climat urbain et la temperature de surface du sol (Mila, Algérie). *Revue Roumaine de Géographie, 64*, 155-174.

Gherraz, H., Guechi, I., & Alkama D. (2020). Quantifying the effects of spatial patterns of green spaces on urban climate and urban heat island in a semi-arid climate. *Bulletin de la Société Royale des Sciences de Liège, 89*, 164-185. https://doi.org/10.25518/0037-9565.9821

Ghosh, S., & Das, A. (2018). Modelling urban cooling island impact of green space and water bodies on surface urban heat island in a continuously developing urban area. *Modeling Earth Systems and Environment, 4*, 501-515. https://doi.org/10.1007/s40808-018-0456-7

Guo, Q., Pu, R., Li, J., & Cheng, J. (2017). A weighted normalized difference water index for water extraction using Landsat imagery. *International Journal of Remote Sensing, 38*, 5430-5445, https://doi.org/10.1080/01431161.2017.1341667

Haashemi, S., Weng, Q., Darvishi, A., & Alavipanah, S. K. (2016). Seasonal variations of the surface urban heat island in a semi-arid city. *Remote sensing, 8*, 352, https://doi.org/10.3390/rs8040352

Hathway, E. A., & Sharples, S. (2012). The interaction of rivers and urban form in mitigating the Urban Heat Island effect: A UK case study. *Building and environment, 58*, 14-22, https://doi.org/10.1016/j.buildenv.2012.06.013

Kabour, A., & Chebbah, L. (2021). Temporal evaluation of the Beni Haroun dam's (Algeria) raw water quality, through a literature review. *Environmental Research and Technology, 6*, 248-257, https://doi.org/10.35208/ert.1287903

Khan, A., & Chatterjee, S. (2016). Numerical simulation of urban heat island intensity under urban–suburban surface and reference site in Kolkata, India. *Modeling Earth Systems and Environment, 2*, 1-11, https://doi.org/10.1007/s40808-016-0119-5

Lee, D., Oh, K., & Seo, J. (2016). An analysis of Urban Cooling Island (UCI) Effects by Water Spaces Applying UCI Indicies. *International Journal of Environmental Science and Development, 7*, 810-815, http://dx.doi.org/10.18178/ijesd.2016.7.11.886

Li, J., Meng, Y., Li, Y., Cui, Q., Yang, X., Tao, C., Wang, Z., Li, L., & Zhang, W. (2022). Accurate water extraction using remote sensing imagery based on normalized difference water index and unsupervised deep learning. *Journal of Hydrology, 612*, Article 128202. https://doi.org/10.1016/j.jhydrol.2022.128202

Manteghi, G., Bin Limit, H., & Remaz, D. (2015). Water bodies an urban microclimate: A review. *Modern Applied Science, 9*(6). https://doi.org/10.5539/mas.v9n6p1

Marouf, N., & Remini, B. (2019). Impact study of Beni-Haroun dam on the environmental and socio-economic elements in Kébir-Rhumel basin, Algeria. *Journal of Water and Land Development, 43*. https://doi.org/10.2478/jwld-2019-0070

Mostofa, T., & Manteghi, G. (2020). Influential factors of water body to enhance the urban cooling islands (Ucis): A review. *International Transaction Journal of Engineering, Management, & Applied Sciences & Technologies, 11*, 1-12. https://doi.org/10.14456/ITJEMAST.2020.27

New, T., & Xie, Z. (2008). Impacts of large dams on riparian vegetation: applying global experience to the case of China's Three Gorges Dam. *Biodiversity and Conservation, 17*, 3149-3163, https://doi.org/10.1007/s10531-008-9416-2

Peng, S., Piao, S., Ciais, P., Friedlingstein, P., Ottle, C., Bréon, F. M., Nan, H., Zhou, L., & Myneni, R. B. (2012). Surface urban heat island across 419 global big cities. *Environmental Science & Technology, 46*, 696-703. https://doi.org/10.1021/es2030438

Sahnoune, S., Benhassine, N., Bourbia, F., & Hadbaoui, H. (2021). Quantifying the effect of green-roof and urban green infrastructure ratio on urban heat island mitigation-semi-arid climate. *Journal of Fundamental and Applied Sciences, 13*, 199-224. https://doi.org/10.4314/jfas.v13i1.12

Shahfahad, Talukdar, S. Rihan, M., Hang, H. T., Bhaskaran, S., & Rahman, A. (2021). Modelling urban heat island (UHI) and thermal field variation and their relationship with land use indices over Delhi and Mumbai metro cities. *Environment, Development and Sustainability, 24*, 3762-3790. https://doi.org/10.1007/s10668-021-01587-7

Stewart, I. D. (2011). A systematic review and scientific critique of methodology in modern urban heat island literature. *International Journal of Climatology, 31*, 200-217, https://doi.org/10.1002/joc.2141

Sun, R., & Chen, L. (2012). How can urban water bodies be designed for climate adaptation? *Landscape and Urban Planning, 105*, 27-33. https://doi.org/10.1016/j.landurbplan.2011.11.018

Syafii, N. I., Ichinose, M., Kumakura, E., Jusuf, S. K., Chigusa, K., & Wong, N. H. (2017). Thermal environment assessment around bodies of water in urban canyons: A scale model study. *Sustainable Cities and Society, 34*, 79-89. https://doi.org/10.1016/j.scs.2017.06.012

Tan, X., Sun, X., Huang, C., Yuan, Y., & Hou, D. (2021). Comparison of cooling effect between green space and water body. Sustainable *Cities and Society, 67*, Article 102711. https://doi.org/10.1016/j.scs.2021.102711

Theeuwes, N. E., Solcerova, A., & Steeneveld, G. J. (2013). Modeling the influence of open water surfaces on the summertime temperature and thermal comfort in the city. *Journal of Geophysical Research: Atmospheres, 118*, 8881-8896. https://doi.org/10.1002/jgrd.50704

Varol, M., Gökot, B., Bekleyen, A., & Şen, B. (2012). Spatial and temporal variations in surface water quality of the dam reservoirs in the Tigris River basin, Turkey. *Catena, 92*, 11-21, https://doi.org/10.1016/j.catena.2011.11.013

Wu, H., Chen, J., Xu, J., Zeng, G., Sang, L., Liu, Q., ... & Ye, S. (2019). Effects of dam construction on biodiversity: A review. *Journal of Cleaner Production, 221*, 480-489. https://doi.org/10.1016/j.jclepro.2019.03.001

Wu, J., Li, C., Zhang, X., Zhao, Y., Liang, J., & Wang, Z. (2020). Seasonal variations and main influencing factors of the water cooling islands effect in Shenzhen. *Ecological Indicators, 117*, Article 106699. https://doi.org/10.1016/j.ecolind.2020.106699

Xie, Q. & Li, J. (2021). Detecting the cool island effect of urban parks in Wuhan: A city on rivers. International *Journal of Environmental Research and Public Health, 18*(1), Article 132. https://doi.org/10.3390/ijerph18010132

Yang, G., Yu, Z., Jørgensen, G., & Vejre, H. (2020). How can urban blue-green space be planned for climate adaption in high-latitude cities? A seasonal perspective. *Sustainable Cities and Society, 53*, Article 101932. https://doi.org/10.1016/j.scs.2019.101932

Zhou, X., Zhang, S., Liu, Y., Zhou, Q., Wu, B., Gao, Y., & Zhang T. (2022). Impact of urban morphology on the microclimatic regulation of water bodies on waterfront in summer: A case study of Wuhan. *Building and Environment, 226*, Article 109720. https://doi.org/10.1016/j.buildenv.2022.109720